Available online at www.sciencedirect.com
ScienceDirect
Optics Communications 277 (2007) 397–405
OPTICS COMMUNICATIONS
www.elsevier.com/locate/optcom

Spot size and radial intensity distribution of focused Gaussian beams in spherical and non-spherical aberration lenses

Abdu A. Alkelly *

Faculty of Science, Department of Physics, Sana'a University, Sana'a, Yemen

Received 10 January 2007; received in revised form 11 May 2007; accepted 14 May 2007

Abstract

We discussed the radial intensity distribution in the presence of spherical aberrations (SA) for cases in which the incident field is a focused Gaussian spot. A numerical solution of a two dimensional integral diffraction (paraxial ray) equation for a relatively large SA is developed by using the well-known trapezoidal rule for integration. The mesh size was chosen so that convergence of the integration is insured to one part in 10^{-8} at successive steps. The spot size and the radial intensity distribution in both SA free lens and lens exhibiting SA are calculated. A relation that determines the spot size at the geometrical focus in aberrated case is developed.

1. Introduction

The increasing importance for studying optical aberration in vision research and the evaluation of the electromagnetic field diffracted by a coherently illuminated circular aperture have been the aim of several research efforts over the last few decades [1–8]. The knowledge of the parameters that characterize the propagation of laser focused Gaussian beams through optical systems and the clear definitions of these parameters have to be the keystone of the optical researchers working with laser beams and they have an important role in the design of optical systems that employ lasers [9–20]. Theoretical studies, dealing with numerical methods by integration of the diffraction integral [1–6,17,19], or by analytical methods by use of a slowly converging infinite series of expansions [9,12,18,20,21], reveal that when a monochromatic converging spherical wave is diffracted by a circular aperture and focused by an ideal lens, the irradiance distribution in the focal region is symmetric about the geometrical focus, and the point of maximum irradiance is located at the focal point. However, if the lens exhibits some aberrations, this will not be the case [1–6]. Many studies on propagation and focusing of Gaussian beams have been done for perfect lenses [9–20], and few of these studies that deal with focusing laser beams by lenses exhibit spherical aberration (SA) [1–6]. However, none of these studies, based on the solutions of Fresnel–Kirchhoff diffraction integral for large (SA), has been presented as a keystone in calculating the Gaussian parameters and the radial intensities distributions of Gaussian beams.

In this paper, we present a clear picture of spot sizes and radial intensities distributions of Gaussian beam behaviours in both a perfect lens and a lens exhibiting relatively large SA. To accomplish this, we will assume that laser beams have transversal dimensions small enough to consider them as paraxial beams. That is, the angular spectrum of the amplitude distribution is located around the axis of propagation, allowing a parabolic approximation for the spherical wave front of the laser beam and, in this approximation, the component of the electric field along the optical axis is neglected. We will take the amplitude of the beams as scalar quantities, which means that the polarization effects are not considered and the beam is assumed complete and homogeneously polarized.

* Tel.: +967 1 261661/267057.
E-mail address: aa_alkelly@yahoo.com

0030-4018/$ - see front matter © 2007 Elsevier B.V. All rights reserved.
doi:10.1016/j.optcom.2007.05.031

2. Theoretical model

We shall consider a circular lens aperture of radius a through which a spherical monochromatic wave of wavelength λ passes from the left and converging towards the axial focal point O, Fig. 1. For paraxial rays, r and the radius of the aperture, a, are very small compared with the distance OC but they are very large compared with the monochromatic wavelength, λ. Therefore, the total amplitude distribution in a given point $P(x,y,z)$ in the plane transversal to the propagation direction due to all elements of area dS surrounding a point Q on the whole wave front W is given by [21]

$$U(P) = -\frac{ik}{2\pi}\frac{e^{-ikf}}{f}\int\int_W A(x,y,z)\frac{e^{iks}}{s}dS \tag{1}$$

where $k = 2\pi/\lambda$ is the wave number, s is the distance between the point of observation, P, and a typical point, Q, on the spherical wave front passing through the center of the aperture. f is the lens focal length and $A(x,y,z)$ stands for the amplitude distribution of the exiting wave field that makes the study of general types of focused fields possible, e.g., diffracted spherical wave in the presence of aberrations and those arising from the focusing of Gaussian beams.

To develop and simplify Eq. (1), we will follow the following steps:

(1) The distance s in the denominator can be replaced by the lens focal length, f, with no appreciable error.
(2) Because the field transmitted by an aperture is cylindrical symmetric, it is convenient to use the cylindrical coordinates (r,θ,z). So, Eq. (1) can be written in the form

$$U(r,\theta,z) = -\frac{i}{\lambda}\frac{\exp(-ika)}{f^2}\int_0^a\int_0^{2\pi} A(r',\theta) \times \exp\left[-i\frac{k}{z}rr'\left(\cos(\theta-\theta')+\frac{1}{2}\right)\right]r'dr'd\theta \tag{2}$$

(3) Under cylindrical symmetry, the two dimensional integration can be reduced to a single-dimensional integration over a cylindrical coordinate r. This occurs by using the formula

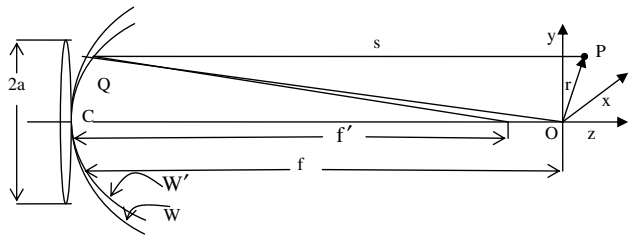

Fig. 1. Diffraction of converging spherical wave at a circular aperture, where W represents a spherical wave due to diffraction which is focused at f, and W' represents a spherical wave due to spherical aberration that is focused at f'. The point P lies in the direct laser beam or in the geometrical shadow.

$$\int_0^{2\pi}\exp\left[-i\frac{k}{z}rr'\cos(\theta-\theta')\right]d\theta = 2\pi J_0\left(\frac{k}{z}rr'\right) \tag{3}$$

where J_0 is the zero-order Bessel function.

(4) We shall consider that the beam diameter coincide with the lens aperture. So, for a single mode laser (TEM_{00}) giving a circular beam of radius a, the Gaussian electric field intensity profile is given by

$$E(r') = E_0\exp\left(-\frac{r'^2}{2a^2}\right), \quad 0 \leqslant r' \leqslant a \tag{4}$$

where r' is the radial distance from the optical axis.

(5) By taking (3) and (4) into account, the spatial variation of intensity can be written in the form

$$I(r,z) = \frac{2\pi a^4 A_0^2}{\lambda^2 f^4} \times \left|\int_0^a \exp\left(-\frac{r'^2}{2a^2}\right)\exp\left(-i\frac{k}{z}\frac{rr'}{2}\right)J_0\left(\frac{k}{z}rr'\right)r'dr'\right|^2 \tag{5}$$

where A_0 is proportional to the maximum amplitude of the wave on the beam axis.

(6) To determine the constant A_0, we can say that the wave front at the lens aperture is physically equivalent to the wave front of the amplitude of wave front over the lens exit pupil A_0/f passing through a filter whose transmission coefficient is a function of the aperture radius, i.e.,

$$E(r') = (A_0/f)T(r')$$

For a Gaussian beam we have

$$T(r') = \exp\left(-\frac{r'^2}{2a^2}\right)$$

And the total energy on an annulus of radius r to $r + dr$ in unit time is

$$dE = 2\pi r'dr'\left(\frac{A_0}{f}T(r')\right)^2 = 2\pi r'dr'\frac{A_0^2}{f^2}\exp\left(-\frac{r'^2}{a^2}\right)$$

The laser beam power is then given by

$$P = \int_0^a dE = \frac{2\pi A_0^2}{f^2}\int_0^a \exp\left(-\frac{r'^2}{a^2}\right)r'dr' = \frac{\pi a^2 A_0^2}{f^2}(1-e^{-1})$$

This means that

$$A_0^2 = \frac{f^2 P}{a^2\pi(1-e^{-1})} \tag{6}$$

where the radius of the laser beam was defined as the radius of the laser beam at the point where the amplitude drops to $(1/e)$ or the intensity drops to $(1/e^2)$.

The intensity distribution in the region of the focus is then given by

$$I(r,z) = \left(\frac{6.33\pi a^2 P}{\lambda^2 f^2}\right) \times \left| \int_0^a \exp\left(-\frac{r'^2}{2a^2}\right) \exp\left\{-\mathrm{i}\frac{k}{z}\frac{rr'}{2}\right\} J_0\left(\frac{k}{z}rr'\right) r'\mathrm{d}r' \right|^2 \quad (7)$$

For a simple biconvex lens of focal length f exhibits only primary spherical aberration, the aberration function is given as [1]

$$\Phi(r) = -0.5a^4\rho^4\left[\frac{n^2}{8(-1)^2}p^3 - \frac{n}{8(n+2)}p^3 + \frac{(n+1)^2}{2(n+2)}p^3\right] \quad (8)$$

where $\rho = a/r$, n is the refractive index of the lens and P is the lens power.

In the presence of the primary spherical aberration, Eq. (7) must be modified to include the extra term, $k\Phi(r)$ and is written in the form

$$I(r,z) = \left(\frac{6.33\pi a^2 P}{\lambda^2 f^2}\right) \times \left| \int_0^a \exp\left(-\frac{r'^2}{2a^2}\right) \times \exp\left\{-\mathrm{i}\frac{k}{z}\left[-\Phi(r) + \frac{rr'}{2}\right]\right\} J_0\left(\frac{k}{z}rr'\right) r'\mathrm{d}r' \right|^2 \quad (9)$$

This is the diffraction equation that we are concerned to solve numerically by using the well-known trapezoidal rule for integration.

3. Numerical solutions and discussion

To ensure that the computer program is both numerically stable and accurately represent the mathematical formulation, we tested it by using several methods. These methods include the selection of the mesh size so that convergence of the integration was insured to 1 part in 10^{-8} at successive steps. This occurs by running the program a number of times at a few points using a steadily decreasing step length until two solutions, using consecutive lengths, are converged. For the reason of rapidly oscillating nature of the integral, it was necessary to use very small step length. Anther test is to compare the numerical results with some analytic known solutions. In all these checks, the computer program presented perfect results. In our work, we assumed a ruby laser of wave length equals to 0.6943 μm incident on a biconvex lens with refractive index $n = 1.5$.

Radial intensities distributions are obtained by setting $z = f$ in Eq. (9). For a lens of 60 mm in focal length and a laser beam diameter of 12 mm, and by assuming aberration free lens, we found that the spot size w_{0p} at $1/e^2$ of the maximum intensity was about 4.4 μm, as we can see from Fig. 2, and is in excellent agreement with the formula [21]

$$w_{0p} = \frac{4\lambda f}{\pi(2a)} \quad (10)$$

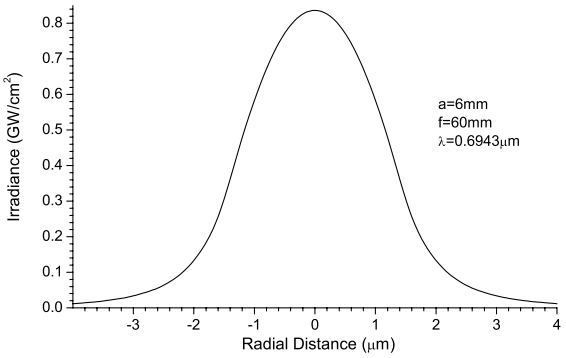

Fig. 2. The radial irradiance distribution of the focused Gaussian beams for SA free lens.

The laser power was 100 W, and the intensity possesses inversion symmetry about the focus. The point of maximum intensity was located at the geometrical focus, at $z = f$, and is equal to 0.836 GW/cm^2.

To show the effects of SA on the spot sizes and the radial distributions of the focused Gaussian beams, we carry out numerical calculations for various beam diameters and lens focal lengths and for the two cases, which are SA free lens and lens exhibiting SA. Fig. 3a illustrates the intensities distributions for a lens of focal length $f = 30$ mm and beam radii $a = 4$, 6, 8, and 10 mm for SA free lens.

The maxima irradiances intensities were, respectively, 1, 3.35, 5.52, and 7.1 GW/cm^2 and, again, they possess inversion symmetry about the focal line and are located at the geometrical focus. The spot sizes w_{0p} were, respectively, 3.28, 2, 1.63 and 1.3 μm and are in a good agreement with the results of Eq. (10) which are, 3.32, 2.2, 1.65 and 1.32 μm, respectively. The results show direct proportionality of the intensity and inverse proportionality of the spot size on the beam diameter. Fig. 3b illustrates the intensities distributions at the best focus for the same values of the parameters of Fig. 3a but now with lens exhibiting SA. The intensities maxima at the best focal point were located far from the geometrical focus toward the lens. The primary spherical aberrations, corresponding to these values of focal lengths, and beam diameters that resulted from Eq. (8) were, respectively, 14λ, 108λ, 456λ and 1395λ. The maxima irradiances densities were, respectively, 29, 32, 33 and 35 MW/cm^2, which are reduced by a factor of 35, 100, 150, and 203, respectively, compared with that of the non-aberrated case, and the distributions possess inversion symmetry about the focal line but the maxima for large SA cases are no longer located at the focal line. We can see that for SA of 108λ, corresponding to beam diameter of 12 mm, the focused intensity diverges from Gaussian significantly and possesses flattened Gaussian shape of size 36 μm, and the larger the beam diameter, which means the larger the SA, the larger the flatness of flattened Gaussian beams, which is in agreement with reference [3]. Furthermore, at a beam diameter of 16 mm, corresponding to SA of about 456λ, the intensity undergoes more divergence from Gaussian shape and it had two maxima, each

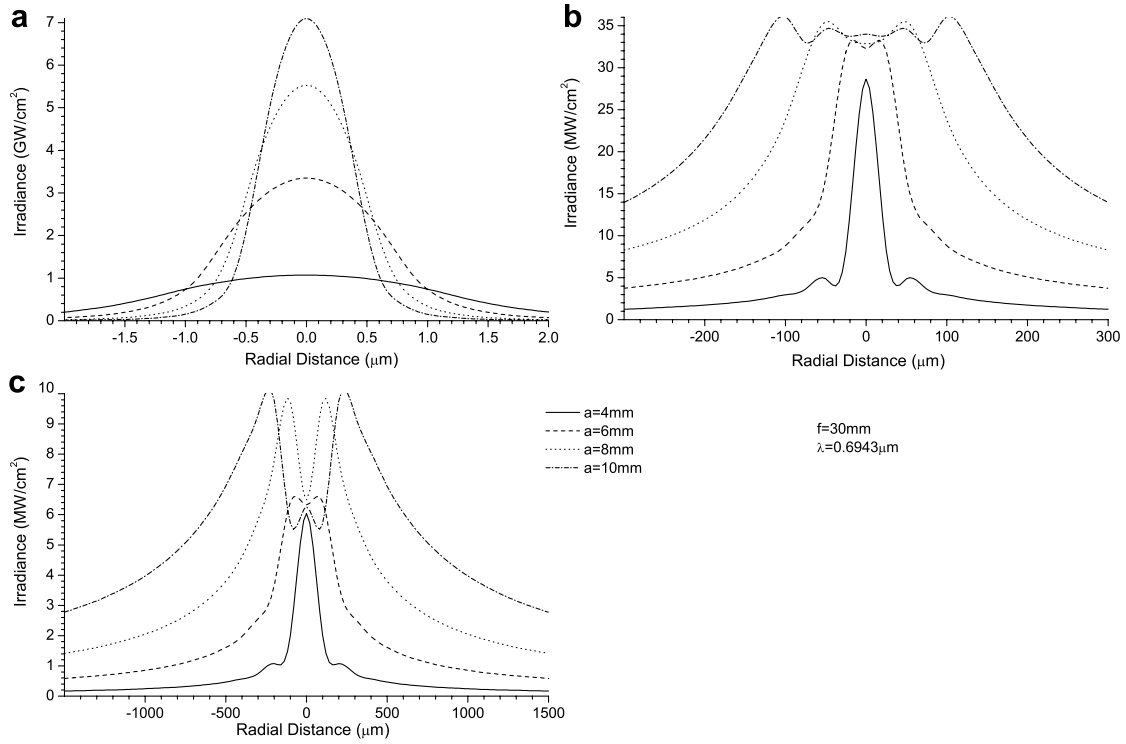

Fig. 3. The radial irradiances distributions of the focused Gaussian beams for different diameters: (a) for SA free lens; (b) for lens exhibits SA, best focus and (c) for lens exhiits SA, geometrical focus.

of them is located at the same distance from the focal line and had flattened Gaussian shape of size 50 μm. The distribution has more divergence at SA of about 1395λ, corresponding to beam diameter of 20 mm, which was of about 210 μm, and some other maxima appeared through this distance but they were very weak. The spot sizes, w_{0Ab}, at $1/e^2$ of the maxima intensities were, respectively, 60, 200, 450 and 880 μm. These results of the spot sizes demonstrate the direct proportionality of the spot sizes on the beam diameters and are in excellent agreement with the relation [22]

$$w_{0Ab} = q\frac{(2a)^3}{f^2} \tag{11}$$

where q is a function of the lens refraction.

Fig. 3c illustrates the intensities distributions at the geometrical focus and, again, for the same values of the parameters of Fig. 3a and with lens exhibits SA. The maxima irradiances intensities were, respectively, 6.04, 6.42, 9.73 and 9.76 MW/cm^2. As we can see, the maxima intensities values are reduced by a factor of 160, 480, 600 and 727, respectively, compared with that of Fig. 3a. The distributions possess inversion symmetry about the focal line but, again, there are some maxima that are no longer located at the focal line and some of the distributions possess flats. For SA of 108λ, corresponding to beam diameter of 12 mm, the distribution had a flattened Gaussian of 320 μm but the peaks intensities at SA of 456λ and at 1395λ have been split into two maxima separated by a distances of 480 and 920 μm, respectively, and are in equal values for each distribution. From the numerical results that were demonstrated in Fig. 3c, the spot sizes w_{0AG} were, respectively, 440, 1500, 3570 and 5580 μm, and are strongly dependent on the beam diameters. From these values of spot sizes we can estimate a relation that allows us to calculate the spot sizes of the intensities distributions at the geometrical focus in aberrated case, which may be written in the form

$$w_{0AG} = \frac{5\pi q}{2}\frac{(2a)^3}{f^2} \tag{12}$$

where q takes the same definition of Eq. (11).

Fig. 4 shows the effect of the beam diameter on the spot sizes in SA free lens and in aberrated case at best focus and at geometrical focus. As we can see, in the case of non-aberrated, the spot sizes are inversely proportional with the beam diameter, Fig. 4a, but in the aberrated case the situation being completely changed, Fig. 4b and c.

To study the effect of the focal length on both the spot sizes and the radial intensities distributions, we continue carrying out numerical calculations for the same beam diameters and for different focal lengths and for the two cases, which are aberrated and non-aberrated.

Fig. 5a illustrates the radial intensities distributions of the focused Gaussian beams for $f = 40$ mm and beam radii $a = 4$, 6, 8, and 10 mm for SA free lens. The maxima irradiances were, respectively, 0.6, 1.88, 3.1, and 4 GW/cm^2 and, again, the intensities distributions possess inversion symmetry about the focus and are located at the geometrical focus. These maxima intensities reduced by nearly a

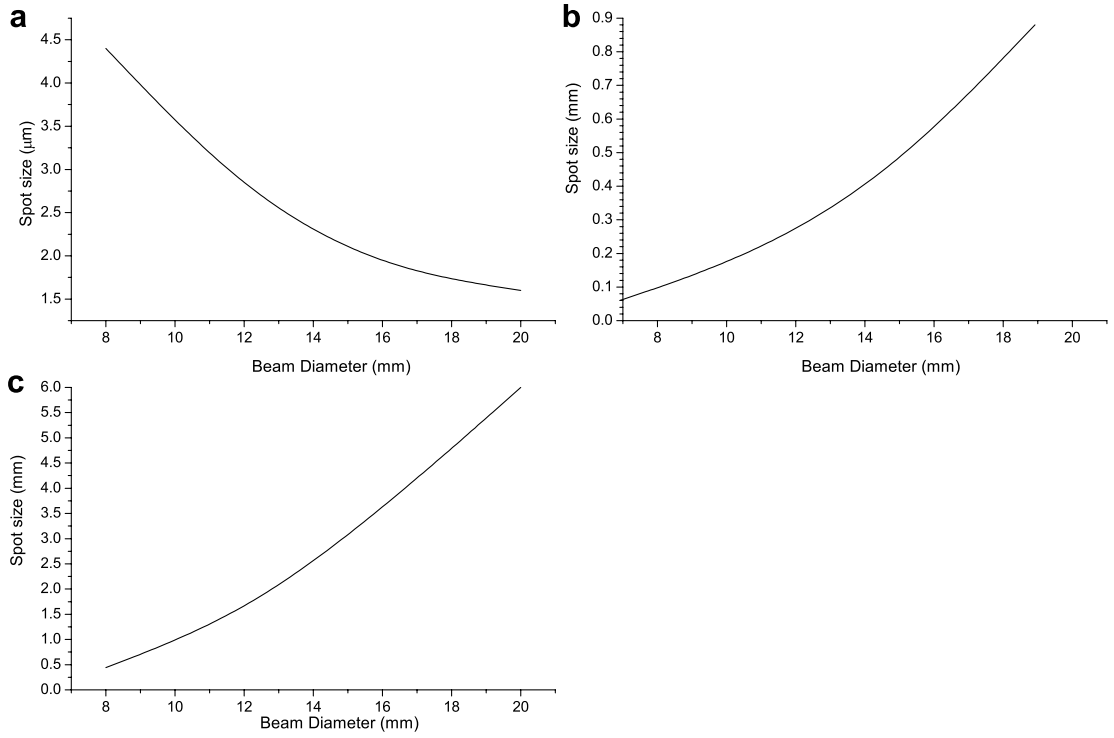

Fig. 4. The relation between beam diameter and spot size: (a) non-aberrated case; (b) aberrated case: at best focus and (c) aberrated case: at geometrical focus.

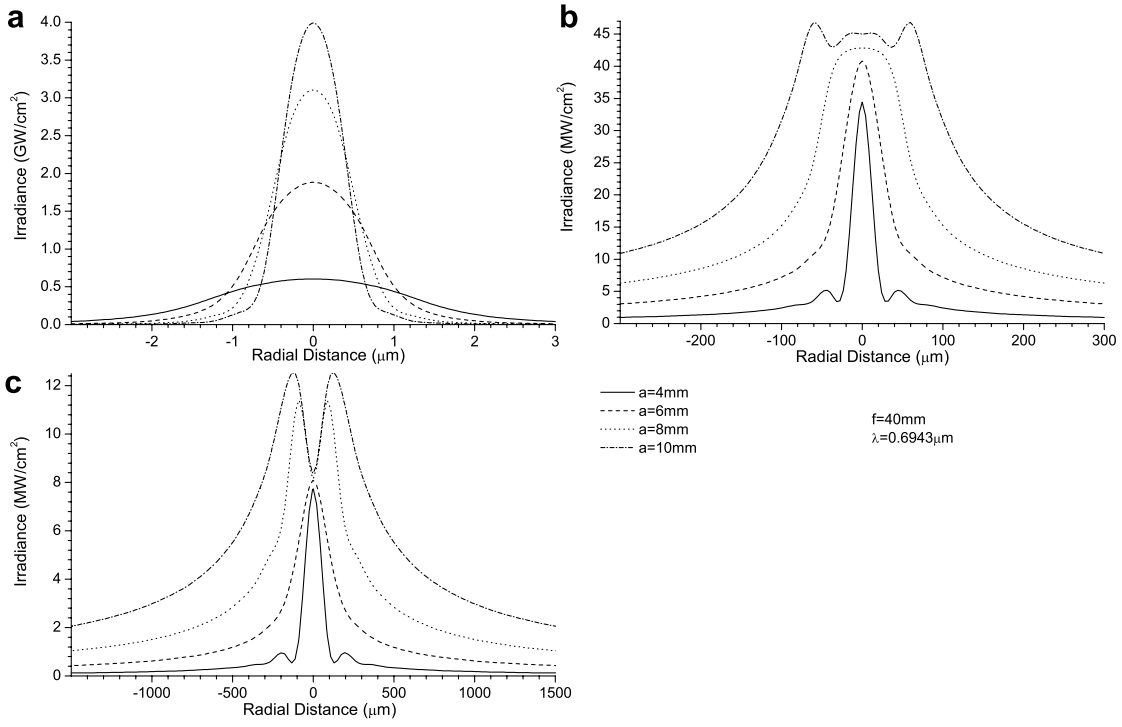

Fig. 5. The radial irradiances distributions of the focused Gaussian beams for different beam diameters: (a) for SA free lens; (b) for lens exhibits SA, best focus and (c) for lens exhibits SA; geometrical focus.

constant factor for all changes in beam diameters which was of about 1.77 in comparison with that of Fig. 3a. The spot sizes, w_{0p} were, respectively, 4.4, 2.85, 2, and 1.6 μm and were in a good agreement with the results of Eq. (10). In addition to the dependency of the intensity on the beam diameter, which is illustrated in Fig. 3a, it is clear now the strong dependence of intensity on the focal length.

The intensities distributions in aberrated case at the best focus for the same values of the parameters of Fig. 5a are understood from Fig. 5b. The primary spherical aberrations corresponding to these values of focal length and beam diameters were, respectively, 6λ, 46λ, 193λ, and 588λ. The maxima irradiances densities were, respectively, 34, 41, 43 and 45 MW/cm^2, which are reduced by a factor of 17.6, 45.8, 72, and 88 compared with the non-aberrated case, Fig. 5a, and increased by a factor of about 1.2 for all changes in beam diameters compared with Fig. 3b. The gain in the intensities comes as a result of increasing the focal length, which reduced the SA. All the distributions possess inversion symmetry about the focal line and the maxima are located at the focal line except the distribution for the diameter of 16, corresponding to SA of 193λ, which is modified to pure flattened Gaussian of about 48 μm and the distribution for the diameter of 20 mm, corresponding to SA of 588λ, which still possesses a flattened Gaussian shape of size 120 μm and contain some weak ripples. The flattened Gaussian shape for diameter 12 mm, corresponding to SA of 46λ that appears in Fig. 3b, is modified to perfect Gaussian shape. The spot sizes, w_{0Ab}, at the same values of the focal length $f = 40$ mm and beam radiuses of 4, 6, 8, and 10 mm were, respectively, 30, 105, 256, and 500 μm and are in good agreement with Eq. (11). Fig. 5c shows the intensities distributions at geometrical focus for the same values of Fig. 5a. The maxima intensities were, respectively, 7.7, 8.1, 11.4, and 12 MW/cm^2, which are smaller by a factor of 78, 232, 271, and 333 compared with that of Fig. 5a, and are larger by a factor of 1.2 for all changes of diameters compared with that of Fig. 3c. The spot sizes were, respectively, 250, 840, 2000, and 3920 μm and are in good agreement with Eq. (12). The intensities distributions possess inversion symmetry about the focal line. The divergence of the distributions from Gaussian shape has been relatively modified at a diameter of 12 mm to pure Gaussian shape, whereas at diameters of 16 and 20 mm, corresponding to SA of 193, and 588λ, the case is still as it is in Fig. 3c. Changes occur only in reducing the distances between the two peaks to 320 and 600 μm respectively.

Fig. 6a illustrates the radial intensities distributions of the focused Gaussian beams for $f = 60$ mm and beam radii $a = 4$, 6, 8, and 10 mm for SA free lens. The maxima irradiances densities were, respectively, 0.268, .836, 1.38, and 1.77 GW/cm^2, which are reduced by nearly a constant factor for all changes in beam diameters, which was of about 2.25 compared with that of Fig. 5a. Again, the distributions possess inversion symmetry about the focal line and are located at the geometrical focus. The spot sizes, w_{0p} were, respectively, 6.8, 4.4, 3.5, and 2.7 μm and are in good agreement with the results of Eq. (10). The intensities distributions in aberrated case at the best focal point for the same values of the parameters of Fig. 6a can be understood from Fig. 6b.

The primary spherical aberrations corresponding to those values of focal lengths and beam diameters were, respectively, 2, 14, 57, and 176λ. The maxima irradiances

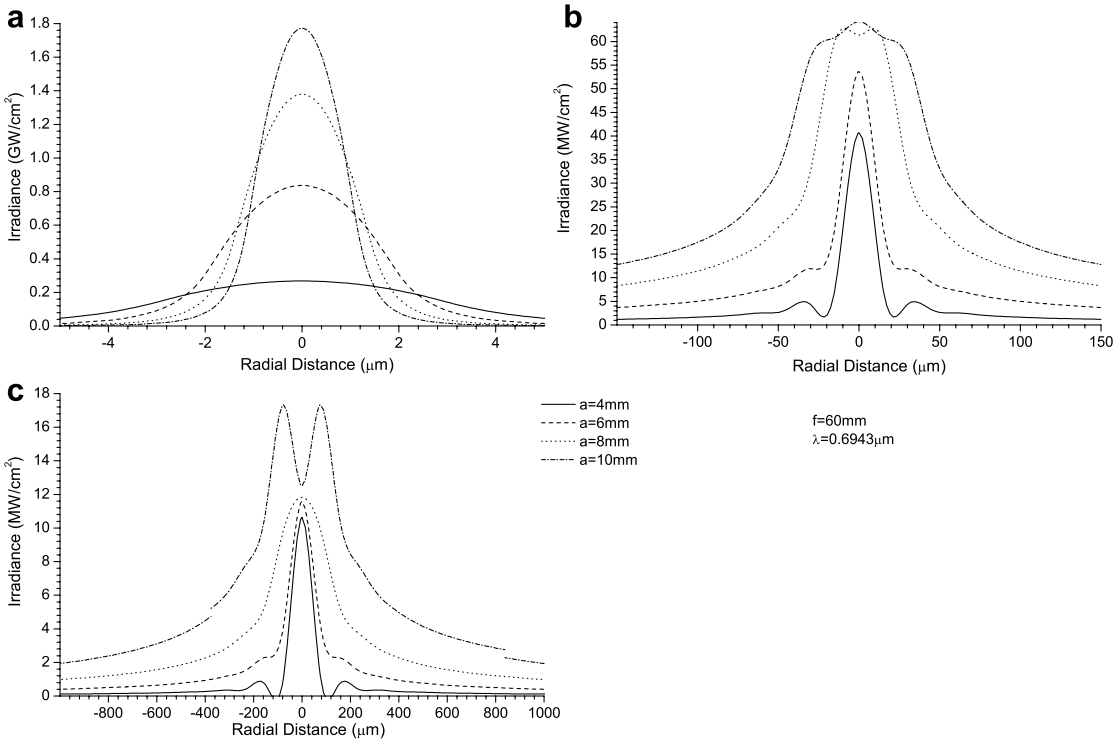

Fig. 6. The radial irradiances distributions of the focused Gaussian beams for different beam diameters: (a) for SA free lens; (b) for lens exhibits SA, best focus and (c) for lens exhibits SA; geometrical focus.

densities were, respectively, 40.1, 54, 61, and 64 MW/cm^2, which are reduced by a factor of 6.7, 15.5, 22.6, and 28 compared with the non-aberrated case, Fig. 6a, and increased by a factor of about 1.32 for all changes in beam diameters compared with Fig. 5b. All the distributions possess inversion symmetry about the focal line, and the flat-

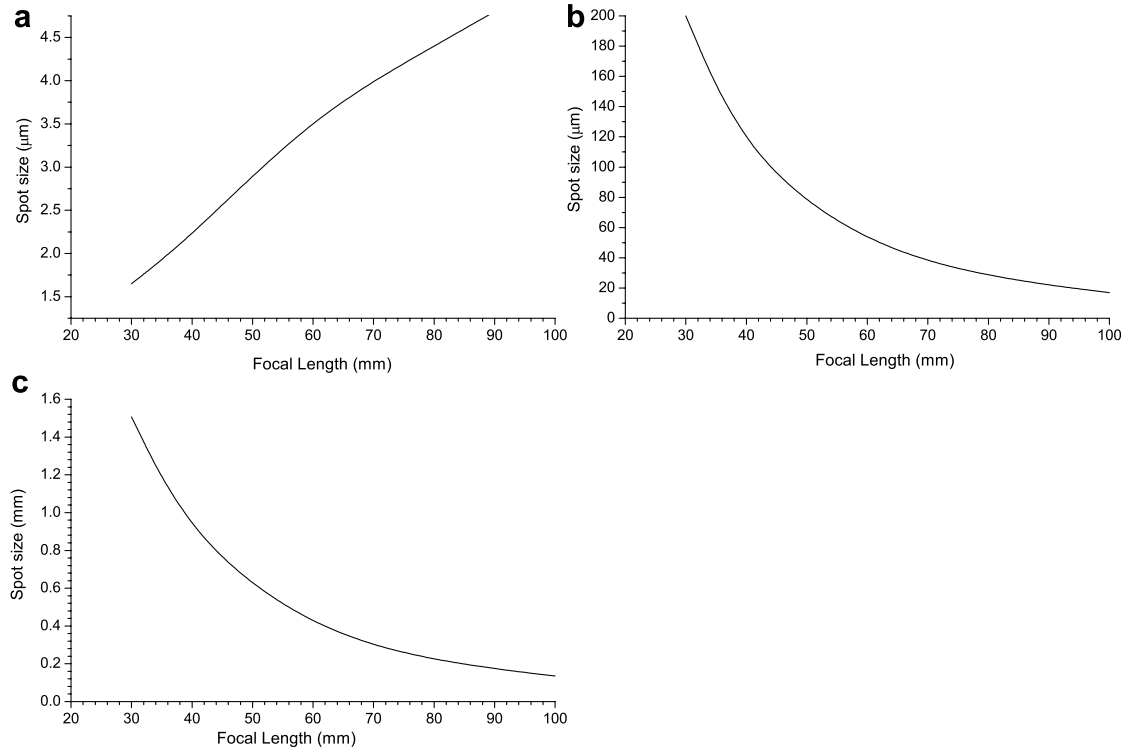

Fig. 7. The radial between focal length and spot size: (a) non-aberrated case; (b) aberrated case: at best focus and (c) aberrated case: at geometrical focus.

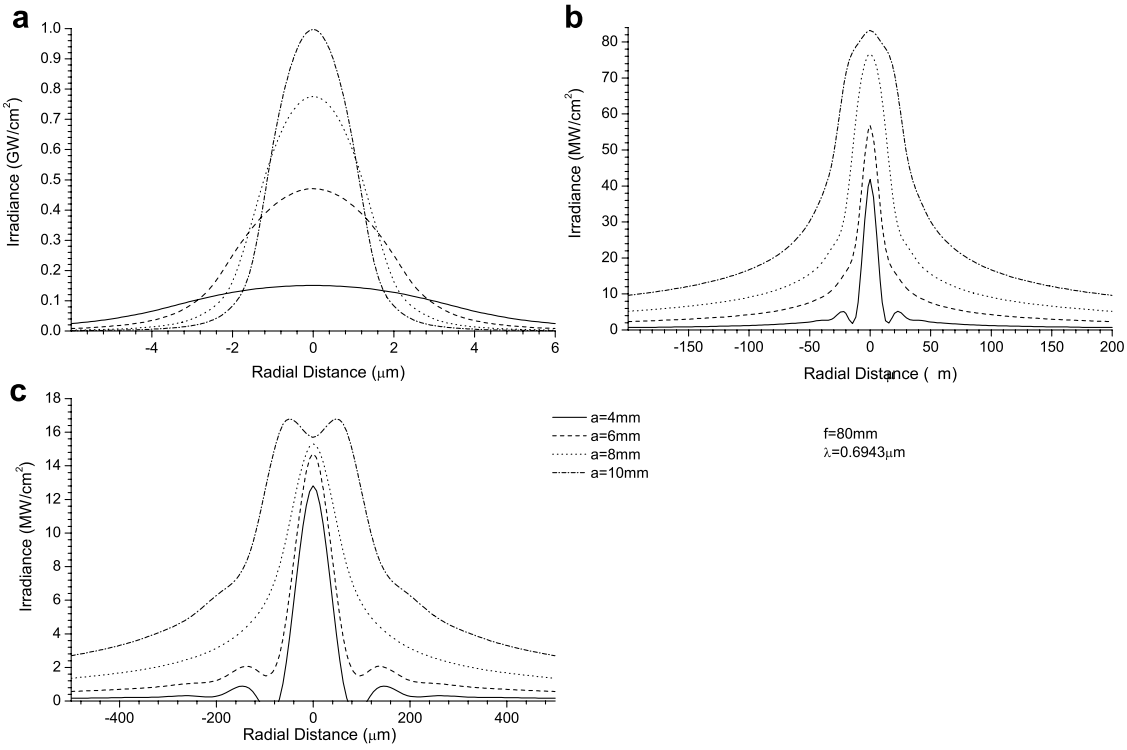

Fig. 8. The radial irradiances distributions of the focused Gaussian beams for different beam diameters: (a) for SA free lens; (b) for lens exhibits SA, best focus and (c) for lens exhibits SA, geometrical focus.

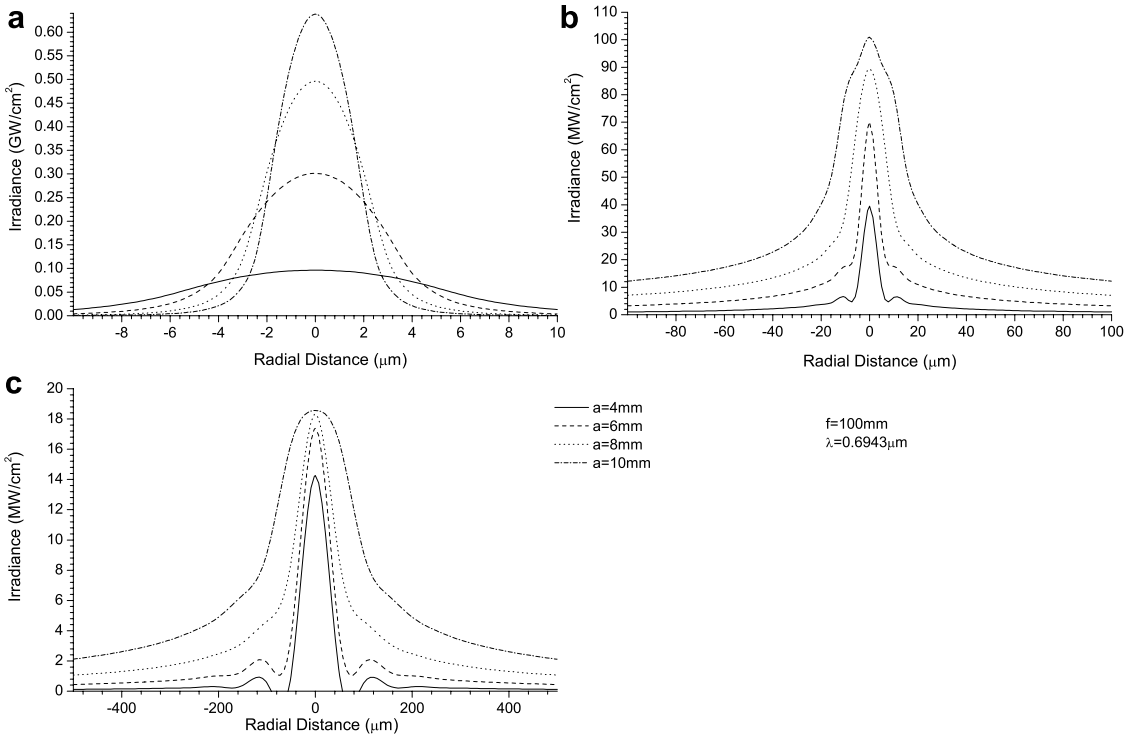

Fig. 9. The radial irradiances distribution of the focused Gaussian beams for different beam diameters: (a) for SA free lens; (b) for lens exhibits SA, best focus and (c) for lens exhibits SA, geometrical focus.

tened Gaussian of the distribution for the diameter of 16 mm corresponding to SA of 57λ has been decreased to 20 μm. The peak of the intensity distribution for the diameter of 20 mm was located at the focal line and has flattened Gaussian at the two sides each of about 22 μm. The spot sizes, w_{0Ab}, at the same values of focal length $f = 60$ mm and beam radii of 4, 6, 8, and 10 mm were, respectively, 14, 48, 114, and 220 μm and are in good agreement with Eq. (11). Fig. 6c shows the intensities distributions at geometrical focus for the same values of Fig. 6a. The maxima intensities were, respectively, 10.6, 11.6, 11.8, and 16.9 MW/cm^2, which are smaller by a factor of 25, 72, 117, and 105 compared with that of Fig. 6a and are larger by a factor of about 1.4 for all diameters compared with that of Fig. 5c. The intensities distributions possess inversion symmetry about the focal line, and the divergence of the distribution from Gaussian shape at diameter of 16 mm, corresponding to SA of 57λ, has been modified to a perfect Gaussian beam whereas the distribution at diameter of 20 mm, corresponding to SA of 176λ, still has two peaks at either sides of the focal line but the distance between them was reduced to 320 μm. The spot sizes, w_{0AG}, for $f = 60$ mm and beam radii of 4, 6, 8, and 10 mm were, respectively, 110, 380, 890, and 1750 μm and are in good agreement with Eq. (12).

The dependency of the spot sizes in non-aberrated and in aberrated cases, at best focus and in geometrical focus on the focal length, are illustrated in Fig. 7. For more knowledge about the effects of increasing the focal length on the radial intensities and spot sizes, we carried out Figs. 8 and 9 for focal lengths of 80 and 100 mm. The general changes were that, at best focus, the divergence from Gaussian shape was modified to perfect Gaussian shape for all distributions, Figs. 8b and 9b. The spot sizes for diameter 8 mm and for focal lengths 80 and 100 mm became aberration limited; and the maximum intensity for diameter 8 mm and for focal length 80 mm amounts 41.8 MW/cm^2, which is larger by a factor of 1.03 in comparison with that of Fig. 6b and is larger by a factor of 1.06 in comparison with that of Fig. 9b. This is because the optimum focal length for beam diameter of 8 mm is about 84 mm. For a geometrical focus, Figs. 8c and 9c, there is no significantly changes except the modification that occurs in the intensity distribution shape for diameter 20 mm, Fig. 8c, which is modified to perfect Gaussian shape, Fig. 9c.

4. Conclusions

The numerical solutions show that when the Gaussian beams are focused by a perfect lens, no SA, the radial intensities distributions possess inversion symmetry about the focal line and the maxima are located at the geometrical focus, and the spot sizes are directly proportional to the lens focal length and inversely proportional to the beam diameter. However, when Gaussian beams are focused by a lens with SA, there are general changes. The results show that the maxima intensities are significantly reduced at both best focus and geometrical focus and the maxima intensities at the geometrical focus were smaller than those

at best focus for all cases under considerations. For large SA, the maxima at both geometrical focus and best focus have been split into two maxima or possess flats, but the distributions still possess inversion symmetry about the focal line. At geometrical focus, the effect of the SA of values greater than 38λ on the radial intensity distribution become very significant, but this value should be greater than 73λ to be very significant at best focuses. The results show that, in contrast with non-aberrated case, the intensities values in the aberrated case are increased with increasing the focal length below the optimum value and then begin to decrease above the optimum focal length. The focused beam radius at the geometrical focus is larger than that of best focus, which is larger than that of non-aberrated case; and the larger the SA the larger the focused beam radius.

References

[1] L.R. Evans, Phys. Med. Beol. 14 (2) (1969) 205.
[2] L.R. Evans, Phys. Rev. Lett. 22 (21) (1969) 1099.
[3] Jixiong Pu, Huihua Zhang, Opt. Commun. 151 (1998) 331.
[4] Baida Lu, Xiaoling Ji, Opt. Commun. 189 (2001) 47.
[5] Christian Parigger, Y. Tang, D.H. Plimmons, J.W.L. Lewis, Appl. Opt. 36 (31) (1997) 8214.
[6] D.P. Biss, T.G. Brown, J. Opt. Soc. Am. 12 (3) (2004) 384.
[7] D. Schurig, D.R. Smith, Phys. Rev. E 70 (2004) 65601-4.
[8] <www.nmr.mgh.Harvard.edu/dessirtation/node79>.
[9] Hakan Urey, Appl. Opt. 43 (3) (2004) 620.
[10] Jianbing J. chen, Tomasz M. Grzegorczyk, Bae-Ian Wu, Jin Au Kong, J. Opt. Soc. Am. 13 (26) (2005) 10840.
[11] Manuel Martinez-Corral, Vicent Climent, Appl. Opt. 35 (1) (1996) 24.
[12] Zapata-Rodregues et al., J. Opt. Soc. Am. A 17 (7) (2000) 1185.
[13] S. De Nicola, D. Anderson, M. Lisak, Pure Appl. Opt. 7 (1998) 1249.
[14] <www.newport.com/servicesupport/Tutorials/default>.
[15] Baohua Jia, Xiaosong Gan, Min Gu, J. Opt. Soc. Am. 13 (18) (2005) 6821.
[16] <http://www.mellesgriot.com/pdf/CatalogX/X_02_2-5.pdf>.
[17] Klaus D. Mielenz, J. Res. Inst. Stand. Technol. 103 (5) (1998) 497.
[18] Manuel Martinez-Corral et al., J. Opt. Soc. Am. A 15 (2) (1998) 449.
[19] D.S. Max, D. Psaltis, J. Opt. Soc. Am. A 14 (6) (1997) 1268.
[20] Carl D. Meinhart, Steven T. Wereley, J. Meas. Sci. Technol. 14 (2003) 1047.
[21] Max Born, Emil Wolf, Principles of Optics, sixth ed., Pergamon press, 1980.
[22] <www.lasercomponents.com>.